



NOVA

University of Newcastle Research Online

nova.newcastle.edu.au

Brown, Jason; Khan, Jamil Y. "Predictive allocation of resources in the LTE uplink based on maximum likelihood estimation of event propagation characteristics for M2M applications" Published in Proceedings of the 2014 IEEE Global Communications Conference (GLOBECOM), p. 4965-4970, (2014)

Available from: <http://dx.doi.org/10.1109/GLOCOM.2014.7037592>

© 2014 IEEE. Personal use of this material is permitted. Permission from IEEE must be obtained for all other uses, in any current or future media, including reprinting/republishing this material for advertising or promotional purposes, creating new collective works, for resale or redistribution to servers or lists, or reuse of any copyrighted component of this work in other works.

Accessed from: <http://hdl.handle.net/1959.13/1337234>

Predictive Allocation of Resources in the LTE Uplink Based on Maximum Likelihood Estimation of Event Propagation Characteristics for M2M Applications

Jason Brown and Jamil Y Khan
School of Electrical Engineering and Computer Science
The University of Newcastle
Callaghan, NSW 2308, AUSTRALIA
Email: {jbrown1, jamil.khan}@newcastle.edu.au

Abstract— We propose a predictive resource allocation scheme for the LTE uplink based upon Maximum Likelihood Estimation of event propagation characteristics for M2M/Smart Grid applications. The LTE eNodeB estimates the inter-sensor propagation time of a disturbance using the pattern and timing of received Scheduling Requests (SRs) from sensors and then proceeds to predict the time at which the disturbance will reach downstream sensors, facilitating predictive uplink grants for these sensors in order to reduce the mean latency of their uplink data packets by up to 50% (according to a performance analysis) compared to the existing standard reactive LTE uplink resource allocation scheme. A further benefit is that when a predictive resource allocation is successful, the sensor does not need to send an SR, thereby freeing up uplink resources which can be critical with M2M communications. We consider various transition strategies from the estimation to prediction phases which reflect the compromise between estimation speed and accuracy, and also examine the concept of early and late prediction.

Index Terms— LTE, M2M, Smart Grid, predictive scheduling, proactive scheduling, OPNET.

I. INTRODUCTION

The data plane latency of the 3GPP Long Term Evolution (LTE) uplink is designed to be less than 10ms in the best case [1]; however, typical latencies can be significantly higher depending upon the system configuration, load, packet size and channel conditions [2]. There is not much opportunity to reduce the uplink latency for traditional voice and data devices which typically act independently of other such devices in the local area. However, for M2M devices acting in a group such as sensors in a Wireless Sensor Network (WSN) in a Smart Grid, the event of one sensor triggering may increase the probability of other sensors in the vicinity also triggering in quick succession. We can exploit these correlated traffic patterns between related devices of the group to reduce latency. This is important because the delay budget in delay sensitive M2M applications such as this can be as low as 10-100ms.

In [3], we introduced a predictive resource allocation scheme in the LTE uplink for event based M2M applications. In the LTE RRC_CONNECTED state [4], a device must normally wait for its assigned periodic SR opportunity in order to request uplink resources from the eNodeB [5][6]. However, if the time remaining to the next SR opportunity is greater than

some threshold determined by the network operator and/or application related to the aggressiveness of the prediction, the eNodeB can in theory assign uplink resources proactively in lieu of waiting to see whether the device actually sends an SR at the designated time. We employed this approach to demonstrate that the mean latency of uplink packets can be reduced by up to 50% under certain circumstances [3]. Note that this scheme represents a “blind” prediction method in which the eNodeB has no knowledge of the underlying correlated traffic characteristics of the group, nor does it attempt to estimate what those patterns are in real time.

A different “non-blind” approach is for the eNodeB to estimate (e.g. using Maximum Likelihood Estimation) the properties of the correlated traffic patterns in real time in order to subsequently predict the future behaviour of downstream devices and proactively assign uplink resources as soon as it is believed data is pending at devices. We investigate this approach in this paper, using a simple M2M application in which a disturbance propagates unidirectionally along a line of equally spaced sensors at a fixed (but unknown) speed. We show that the approach is low complexity, scalable and can reduce the mean latency of the uplink data packets by up to 50% for an example scenario compared to the existing standard reactive LTE uplink resource allocation scheme. This is in spite of the fact that the prediction phase cannot begin until the estimation phase has completed, which is a major disadvantage compared to the blind approach. We consider various transition strategies from the estimation to prediction phases which reflect the compromise between estimation speed and accuracy, and also examine the concept of early and late prediction.

Any form of predictive uplink resource allocation is subject to wastage of resources in the case when a predictive resource allocation is made, but there is currently no data pending at the target device. The counter argument is that when a successful prediction occurs, not only is latency generally reduced, but the target device does not need to send an SR, thereby reducing uplink control channel resource usage.

There is some related work in the literature. In [7], a predictive scheduling algorithm for uplink traffic in IEEE 802.16 networks is described which aims to reduce latency for the real time polling service (rtPS) based upon analysis of the bandwidth request queues at the base station, although this

work does not exploit the correlated traffic patterns associated with some M2M applications. In [8-9], the authors define proactive/predictive resource allocation for wireless networks at the single user level in order to afford delay and capacity gains. In contrast, our work addresses predictive resource allocation at the group level.

II. EVENT PROPAGATION ESTIMATION AND PREDICTION

A. Principles

Consider a simple abstract M2M application in which a group of LTE capable sensor nodes in the RRC_CONNECTED state which send data on certain events are equally spaced along a line. Now consider a disturbance travelling unidirectionally along the line at a fixed speed (at least locally) such that the disturbance requires an unknown duration τ to travel between contiguous nodes. When the disturbance reaches a node, that node waits for its next preassigned periodic Scheduling Request (SR) opportunity to send an SR to the eNodeB. In this section, we show how the eNodeB can exploit the timing and sequence of the received SRs to develop an estimator for τ assuming knowledge of the relative locations of nodes (through either static provisioning or dynamic registration). This estimator can be employed to predict when the disturbance will reach more distant sensors and ultimately to facilitate timely proactive uplink resource allocation for such sensors so that data can be transferred with the minimum latency. The estimation process is non-trivial because the nodes do not necessarily send SRs in the same order (or with the same relative timing) in which the disturbance reaches them.

Fig. 1 demonstrates the background to the estimation and prediction processes.

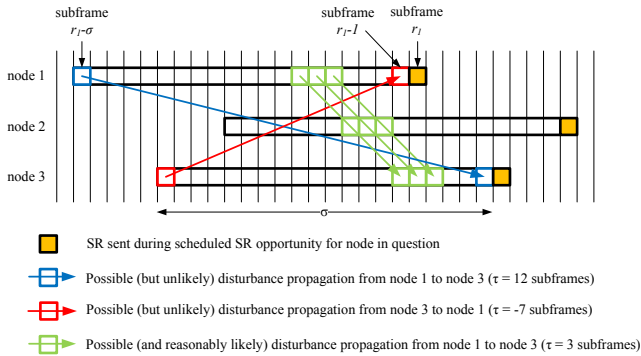


Fig. 1: Possible Disturbance Profiles Based on SR Timing

Each of the three example nodes sends an SR during its first pre-assigned node specific SR opportunity after the disturbance has reached it. SR opportunities occur periodically with a period σ subframes where σ is an eNodeB configuration parameter (equal to one of 5, 10, 20, 40 or 80ms). This implies that the disturbance reached the node sometime within the σ subframes immediately preceding the sending of the SR (assuming that a node cannot detect the disturbance and send an SR in the same subframe). For example, node 1 sent its SR in subframe r_1 , therefore the disturbance reached node 1 during subframe T_1 where $r_1 - \sigma \leq T_1 \leq r_1 - 1$. In fact each of these possible values of the random variable T_1 is equally likely, so

$T_1 \sim \text{Uniform}(r_1 - \sigma, r_1 - 1)$. The possible values of T_1 (and also T_2 and T_3 for nodes 2 and 3 respectively) are indicated by rectangles in Fig. 1.

There are a wide range of possible disturbance profiles that can satisfy the observed timing of SRs subject to the constraint that $T_3 = T_2 + \tau = T_1 + 2\tau$ where τ can be positive or negative (but is assumed to be an integer number of subframes) as indicated in Fig. 1. However, it is clear that some values of τ are more likely than others and we can therefore derive a maximum likelihood estimator for τ .

B. Maximum Likelihood Estimation for τ

For simplicity, we will consider a group of n adjacent nodes labelled $1, 2 \dots n$ which have recently sent SRs during subframes $r_1, r_2 \dots r_n$ respectively such that $T_1 = t_1, T_2 = t_2 \dots, T_n = t_n$ in this section. The analysis also applies to the more general case in which the group of n nodes are not adjacent i.e. there are one or more intermediate nodes that have not recently sent SRs. The likelihood $\mathcal{L}(\tau | t_1, t_2 \dots t_n)$ as a function of τ is defined as:

$$\mathcal{L}(\tau | t_1, t_2 \dots t_n) = \Pr(t_1, t_2 \dots t_n | \tau) = f(t_1, t_2 \dots t_n | \tau) \quad (1)$$

where $f(T_1, T_2 \dots T_n | \tau)$ is the joint probability mass function of $T_1, T_2 \dots T_n$.

The random variables $T_1, T_2 \dots T_n$ are in fact completely dependent upon each other as follows:

$$T_m = T_{m-1} + \tau \quad (2)$$

or alternatively:

$$T_m = T_1 + (m - 1)\tau \quad (3)$$

As a result, Eq.(1) can be re-written as:

$$\begin{aligned} \mathcal{L}(\tau | t_1) &= \Pr(t_1, t_1 + \tau \dots t_1 + (n - 1)\tau | \tau) \\ &= f(t_1, t_1 + \tau \dots t_1 + (n - 1)\tau | \tau) \end{aligned} \quad (4)$$

Using the chain law of probability:

$$\mathcal{L}(\tau | t_1) = \Pr(T_1 = t_1) \prod_{i=2}^n \Pr(T_i = t_i + (i - 1)\tau | T_{i-1} = t_{i-1} + (i - 2)\tau \dots T_1 = t_1) \quad (5)$$

Summing over all possible values of T_1 and using the fact that $\Pr(T_1 = t_1) = 1/\sigma$ given that $T_1 \sim \text{Uniform}(r_1 - \sigma, r_1 - 1)$:

$$\mathcal{L}(\tau) = \frac{1}{\sigma} \sum_{t_1=r_1-\sigma}^{r_1-1} \prod_{i=2}^n \Pr(T_i = t_i + (i - 1)\tau | T_{i-1} = t_{i-1} + (i - 2)\tau \dots T_1 = t_1) \quad (6)$$

The conditional probability $\Pr(T_i = t_i + (i - 1)\tau | T_{i-1} = t_{i-1} + (i - 2)\tau \dots T_1 = t_1)$ is evaluated as follows:

$$\Pr(T_i = t_i + (i - 1)\tau | T_{i-1} = t_{i-1} + (i - 2)\tau \dots T_1 = t_1)$$

$$= \begin{cases} 1, & r_i - \sigma \leq t_1 + (i-1)\tau \leq r_i - 1 \\ 0, & \text{otherwise} \end{cases} \quad (7)$$

since $T_i = t_1 + (i-1)\tau$ is only feasible if it falls within the σ subframes immediately preceding r_i , the subframe in which node i sends its SR.

We can simplify Eq. (6) and Eq. (7) by considering a derived random variable U_m as follows:

$$U_m = T_m - (m-1)\tau \quad (8)$$

such that Eq. (6) becomes:

$$\mathcal{L}(\tau) = \frac{1}{\sigma} \sum_{t_1=r_1-\sigma}^{r_1-1} \prod_{i=2}^n \Pr(U_i = t_1 \mid U_{i-1} = t_1 \dots U_1 = t_1) \quad (9)$$

and Eq. (7) becomes:

$$= \begin{cases} 1, & r_i - \sigma - (i-1)\tau \leq t_1 \leq r_i - 1 - (i-1)\tau \\ 0, & \text{otherwise} \end{cases} \quad (10)$$

Intuitively, one interpretation of Eq. (8), Eq. (9) and (10) involves shifting the interval (as defined by the rectangle) of node m in Fig. 1 by $-(m-1)\tau$ subframes and then calculating the overlap between the shifted intervals as illustrated in Fig. 2 for the example case of $\tau = 2$ subframes.

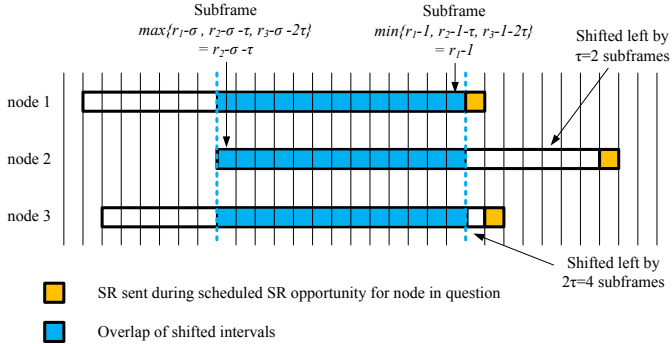


Fig. 2: Calculating Likelihood using Overlap of Shifted Intervals (assumes $\tau=2$ subframes)

The advantage of this interpretation is that we can derive a simple equation for $\mathcal{L}(\tau)$ that only involves the endpoints of the shifted intervals as follows:

$$\mathcal{L}(\tau) = \begin{cases} \frac{a-b+1}{\sigma} = \frac{c}{\sigma}, & a \geq b \\ 0, & a < b \end{cases} \quad (11)$$

$$a = \min\{r_1 - 1, r_2 - 1 - \tau, \dots, r_n - 1 - (n-1)\tau\}$$

$$b = \max\{r_1 - \sigma, r_2 - \sigma - \tau, \dots, r_n - \sigma - (n-1)\tau\}$$

where the $\min\{\}$ and $\max\{\}$ functions define the minimum and maximum values respectively of the arguments in the braces. Eq. (11) is justified because the upper limit of the overlap

interval is defined by a and the lower limit of the overlap interval is defined by b as demonstrated in Fig. 2, so the likelihood is given by normalising the number of overlapping subframes $c = a - b + 1$ assuming $a \geq b$.

For given values of $r_1, r_2 \dots r_n$, we select the value of $\tau = \hat{\tau}$ which maximizes the likelihood $\mathcal{L}(\tau)$ in Eq. (11). The low complexity of the likelihood calculation leads to a scalable solution. In this paper, we perform this estimation via maximization numerically since it is relatively simple in nature. However, we note that for the trivial case of just 2 nodes, l and m , which have sent SRs during subframes r_l and r_m respectively, there is a closed form algebraic solution for the MLE of $\hat{\tau}$ as follows:

$$\hat{\tau} = \frac{r_m - r_l}{m - l} \quad (12)$$

It is an ongoing research item to discover whether a more general closed form algebraic solution exists for the maximum likelihood estimate $\hat{\tau}$.

With reference to Eq. (11), when a maximum likelihood estimate $\hat{\tau}$ is chosen such that $\mathcal{L}(\hat{\tau}) = c/\sigma$, there are c possible values for T_1 (and all other T_m for $m > 1$ courtesy of Eq. (3)). This is important because, for the purposes of predicting when the disturbance will reach more distant nodes, we must select one of these possible values for T_1 . There are different strategies here, including early and late prediction. We might also desire in principle to achieve a maximum likelihood estimate $\hat{\tau}$ such that $c = 1$ and $\mathcal{L}(\hat{\tau}) = 1/\sigma$ since then there is only one possible value for each of the random variables $T_1, T_2 \dots T_n$ and the prediction can be conducted very accurately.

Fig. 3 illustrates the maximum likelihood estimate $\hat{\tau}$ for $n \geq 2$ selected by maximizing the likelihood $\mathcal{L}(\tau)$ in Eq. (11) for simulations involving $\sigma = 40$ subframes, $\tau = 10ms$ and SR offsets for the various nodes which are identically and independently distributed according to a discrete uniform distribution across the SR period. For a given value of n , if more than one estimate of τ results in the same maximum likelihood, the highest such estimate is chosen. The rationale for this is that it is better to select an estimate for τ which is too high (and results in a predictive resource allocation which occurs after a scheduled SR at a target node and therefore can be cancelled) than one which is too low (and results in a predictive resource allocation which occurs too early before data is available at a target node and thereby wastes resources). Clearly the estimates of τ can be very inaccurate for small values of n , but convergence to the true value of τ generally occurs for $n < 25$ for this set of parameters.

Fig. 4 depicts the maximum likelihood values used to select the maximum likelihood estimate $\hat{\tau}$ in Fig. 3. With reference to Eq. (11), as n increases, the number c of distinct possible values of $T_1, T_2 \dots T_n$ is reduced, and therefore the maximum likelihood also decreases. For $n = 2$, assuming the two nodes sending SRs are adjacent, there are $c = \sigma$ possible values of T_1 and T_2 corresponding to the maximum likelihood estimate $\hat{\tau}$, and therefore the maximum likelihood equals 1. For large n , we reach the point where there is only a single possible set of

values of $T_1, T_2 \dots T_n$ corresponding to the maximum likelihood estimate $\hat{\tau}$, therefore $c = 1$ and the maximum likelihood drops to its minimum value of $1/\sigma$. From Fig. 4, it can be seen that the maximum likelihood first drops to $1/\sigma$ (0.025 for $\sigma = 40$ subframes) between $n = 50$ (for run 3) and $n = 88$ (for run 1). These are much higher values of n than required to obtain a stable and accurate estimate of τ .

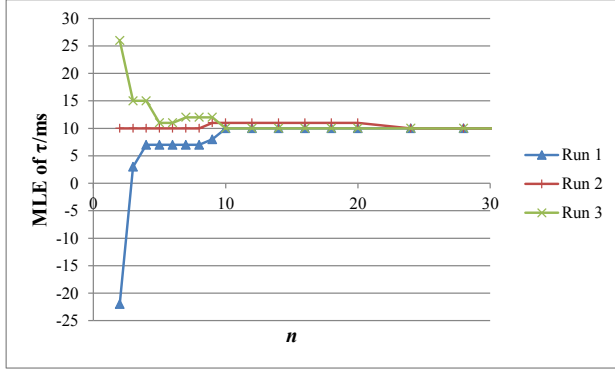


Fig. 3: Maximum Likelihood Estimate $\hat{\tau}$ versus n ($\sigma=40$ subframes, $\tau=10\text{ms}$)

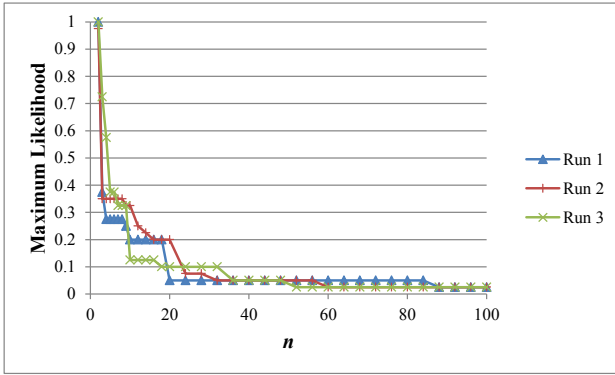


Fig. 4: Maximum Likelihood versus n ($\sigma=40$ subframes, $\tau=10\text{ms}$)

C. Transition Between Estimation and Prediction

The choice of value for n for which the eNodeB scheduler should transition between estimation and prediction is a compromise. On the one hand, we prefer n to be sufficiently high that the maximum likelihood estimate $\hat{\tau}$ is very accurate and the number of possible values of $T_1, T_2 \dots T_n$ is very small so that we can perform prediction for more distant nodes accurately. On the other hand, waiting for n to reach such a high value reduces the scope for predictive resource allocation gains since there are fewer target nodes for predictions.

In order to assess various transition strategies, we define the estimation error e as follows:

$$e = \hat{\tau} - \tau \quad (13)$$

Table I provides a comparison of several example transition strategies in terms of the sample mean error \bar{e} , the sample mean squared error \bar{e}^2 and sample mean minimum number of nodes \bar{n}_{min} that need to send an SR to satisfy the transition criterion, as determined through simulation. The *Run*(x) criterion refers

to finding the first run of x identical values of $\hat{\tau}$ as n increases. Table I clearly demonstrates the compromise between low estimation error and high values of \bar{n}_{min} . We consider these transition strategies in the prediction stage to understand the impact on key performance metrics such as packet latency.

Table I: Sample Transition Strategies and Associated Performance Metrics ($\sigma=40$ subframes, $\tau=10\text{ms}$)

Transition Criterion	\bar{e}	\bar{e}^2	\bar{n}_{min}
$\mathcal{L}(\hat{\tau}) = 1/\sigma$	0.00	0.00	62.49
$\mathcal{L}(\hat{\tau}) \leq 4/\sigma$	0.02	0.12	21.20
$\mathcal{L}(\hat{\tau}) \leq 8/\sigma$	0.05	0.69	13.24
Run(7)	-0.18	0.44	15.53
Run(5)	-0.53	1.91	11.96
Run(3)	-0.80	6.68	6.88

D. Prediction

At its very simplest, prediction is a one-time activity at the eNodeB scheduler following transition from the estimation phase in which we use the maximum likelihood estimate $\hat{\tau}$ and one of the c remaining possible values of T_1 (denoted here as \hat{T}_1) where $c = \mathcal{L}(\hat{\tau})\sigma$ from Eq. (11) to determine the complete set of values $\{\hat{T}_m\}$ according to a variant of Eq. (3) as follows:

$$\hat{T}_m = \hat{T}_1 + (m - 1)\hat{\tau} \quad (14)$$

For each node m which has not already sent an SR in response to the disturbance, we then provisionally schedule a predictive uplink grant to occur at subframe $\hat{T}_m + 1$ unless this occurs in the past, in which case the predictive uplink grant is instead provisionally scheduled for the very next subframe in the future. However, if this predictive resource allocation conflicts with an existing SR opportunity for the node in question, it is cancelled since there is little to be gained relative to the existing reactive resource allocation scheme.

We distinguish between *early* prediction in which \hat{T}_1 is set to the minimum of the c remaining possible values of T_1 and *late* prediction in which \hat{T}_1 is set to the corresponding maximum value of T_1 . Intuitively we expect early prediction to result in a higher probability of unsuccessful prediction. For the $\mathcal{L}(\hat{\tau}) = 1/\sigma$ transition criterion, there is by definition only one remaining possible value of T_1 for the chosen value of $\hat{\tau}$; therefore in this case early and late prediction are identical.

In a practical system, it is likely that there would be continued re-estimation and re-prediction after the initial estimation to prediction transition. This would compensate for changes in the speed of the disturbance and/or correct errors in the initial estimation. However, we do not consider such a closed loop control system in this initial paper.

III. SIMULATION

A. Simulation Model

We make use of a simple M2M application model in which a disturbance propagates unidirectionally along a line of 200 equally spaced LTE enabled sensors at a fixed (but initially unknown) speed. In each simulation run, the disturbance starts at a random position along the first half of the line and travels

the complete length of the line, resulting in sensors sending SRs and data packets in response to detecting the disturbance. The sensors are assigned random offsets (according to a discrete uniform distribution) within the SR period.

The eNodeB scheduler calculates a maximum likelihood estimate $\hat{\tau}$ of the inter-sensor propagation time for each successive SR received as per Section II.B, and based upon a given estimation to prediction transition criterion, ultimately ceases the estimation procedure and proceeds to a one-shot uplink predictive resource allocation for all sensors that have not already sent SRs in response to the disturbance as per Section II.D. It is recognised that the relative performance of the various transition criteria depends upon the number of sensors (since the different criteria require a different mean number of SRs in order for transition to be triggered), so the results of the simulation are not universal, but rather aim to clarify the important aspects of the proposed predictive resource allocation scheme.

Simulations are conducted using a custom OPNET model.

B. Simulation Parameters

Table II lists the OPNET simulation parameters.

Table II: Simulation Parameters

Parameter	Value
Frequency Band	3GPP Band 1 (1920MHz uplink / 2110MHz downlink)
Mode	FDD
Channel bandwidth	2x5MHz
Cyclic prefix type	Normal
Maximum device Tx power	1W
Maximum eNodeB Tx power	5W
Device Rx sensitivity	-110dBm
eNodeB Rx sensitivity	-123dBm
Device antenna gain	0dBi for closest 150 sensors to eNodeB, 4dBi for other 50 sensors
eNodeB antenna gain	9dBi
Device height	1.5m
eNodeB height	40m
SR periodicity σ	40ms
PUCCH channels	2
Channel models	Suburban fixed Erceg model with Terrain Type C
HARQ	Supported
Radio access network model	Single cell, 5km radius (78.5km ²)
Packet size	32 bytes (application layer) 60 bytes (IP layer)
QoS for uplink/downlink traffic	Best effort on default bearer
Uplink/downlink scheduler algorithm	Dynamic fairness (initial uplink allocation of 504 bits at the application layer)
Inter-sensor propagation time τ	10ms

IV. RESULTS

Fig. 5 illustrates the mean delay for all uplink packets and for uplink packets corresponding to successful predictive resource allocations for the various transition strategies and late as opposed to early prediction. Results for a reference no prediction scenario are also included. It can be seen that all the transition strategies result in some reduction of mean delay for all uplink packets relative to the no prediction scenario. In particular, the $\mathcal{L}(\hat{\tau}) = 1/\sigma$, $\mathcal{L}(\hat{\tau}) \leq 4/\sigma$ and Run(7) transition

strategies result in almost a 50% reduction in mean uplink delay (from 26ms to approximately 14ms) for this example simulation scenario. The $\mathcal{L}(\hat{\tau}) = 1/\sigma$ transition strategy supports a mean delay for uplink packets corresponding to successful predictive resource allocations of approximately 6ms (which is the minimum uplink access delay possible in the existing LTE reactive uplink access mechanism [2][3]) due to the high accuracy of its estimation and prediction phases. The mean uplink delay for successful predictions for other transition strategies is higher because of the lower accuracy of the associated estimation and prediction processes.

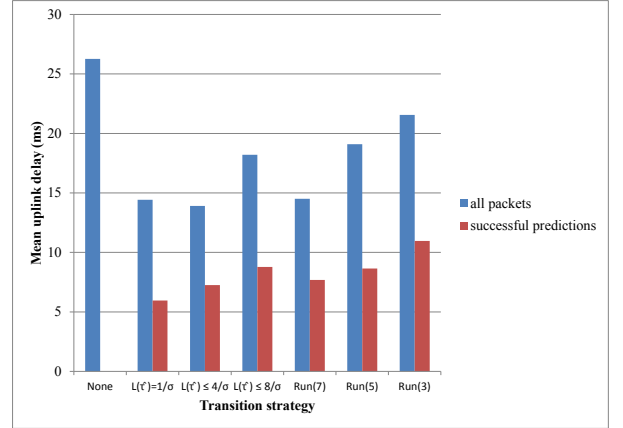


Fig. 5: Mean Uplink Delay for Various Transition Strategies and Late Prediction

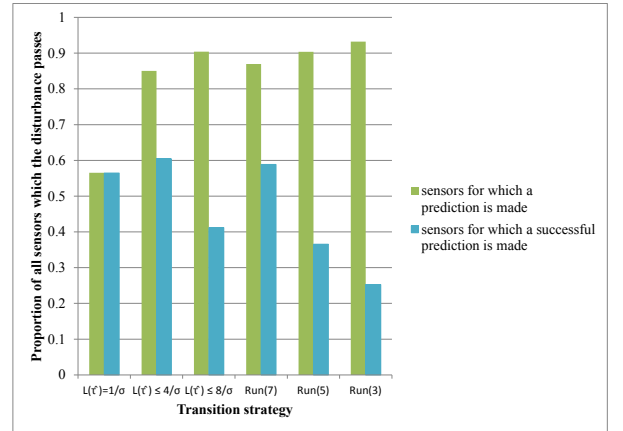


Fig. 6: Proportion of Sensors with Certain Prediction Outcomes for Various Transition Strategies and Late Prediction

Fig. 6 illustrates the proportion of all sensors which the disturbance passes for which a (successful) prediction is made for the various transition strategies and late as opposed to early prediction. It is clear that the proportion of sensors for which a prediction is made is significantly lower for the $\mathcal{L}(\hat{\tau}) = 1/\sigma$ transition strategy than the other transition strategies. This is because the $\mathcal{L}(\hat{\tau}) = 1/\sigma$ transition strategy takes significantly longer on average to complete its estimation procedure and transition to the prediction stage, so that although the estimation is more accurate (and there is a 100% success rate on predictions), there are fewer remaining sensors on which to perform a prediction. This also explains why the $\mathcal{L}(\hat{\tau}) = 1/\sigma$

transition strategy does not outperform some other transition strategies in relation to the mean delay for all uplink packets in Fig. 5. Note the correlation between the fact that the $\mathcal{L}(\hat{\tau}) = 1/\sigma$, $\mathcal{L}(\hat{\tau}) \leq 4/\sigma$ and Run(7) transition strategies have the highest proportion of successful predictions in Fig. 6 and also the lowest mean delay for all uplink packets in Fig. 5. The proportion of sensors for which a successful prediction is made is also a measure of the uplink control channel resources which are saved due to the fact that an SR does not need to be sent.

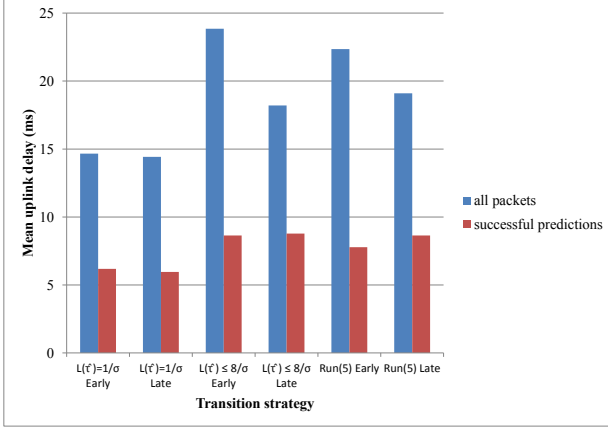


Fig. 7: Mean Uplink Delay for Early and Late Prediction

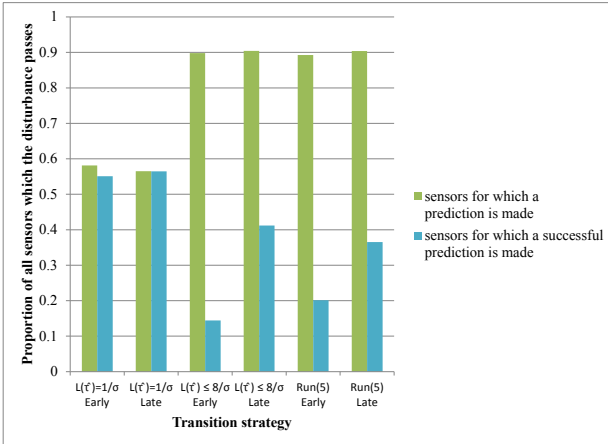


Fig. 8: Proportion of Sensors with Certain Prediction Outcomes for Early and Late Prediction

Fig. 7 and Fig. 8 compare the performance of early and late prediction in terms of mean uplink delay and the proportion of all sensors which the disturbance passes for which a (successful) prediction is made respectively. Clearly, as expected, the performance of the $\mathcal{L}(\hat{\tau}) = 1/\sigma$ transition strategy is almost identical for early and late prediction because there is only a single possible value of T_1 when the transition to the prediction phase occurs. In contrast, late prediction outperforms early prediction for the $\mathcal{L}(\hat{\tau}) \leq 8/\sigma$ and Run(5) transition strategies. In particular, the mean delay for all uplink packets is significantly lower for late prediction due to the fact that the proportion of sensors for which a successful prediction occurs is significantly higher. This reflects the fact that there are usually multiple possible values of T_1 when the transition to

the prediction phase occurs with these transition strategies, so the choice of \hat{T}_1 is significant.

V. CONCLUSIONS

In this paper, we have proposed a predictive resource allocation scheme employed at the eNodeB for the LTE uplink based on maximum likelihood estimation of event propagation characteristics for M2M applications. The eNodeB first attempts to estimate the inter-sensor propagation time τ of a disturbance based upon the timing of received Scheduling Requests (SRs) from sensors using an interval overlapping maximization algorithm. It transitions from the estimation to the prediction phase when a certain criterion based upon likelihood or a run in stable values of τ is triggered. During prediction, the eNodeB schedules uplink grants for sensors which have not already sent an SR in response to the disturbance using either early or late prediction.

Initial simulation results demonstrate that the mean latency of uplink packets can be reduced by up to 50% depending upon the estimation to prediction transition strategy, with late prediction usually outperforming early prediction. There is also a compromise between obtaining maximum accuracy in the estimation process (which requires the disturbance to pass more sensors before transitioning to the prediction phase) and transitioning to the prediction phase earlier with a lower accuracy estimate in order to increase the number of remaining sensors for which predictions can be made. We intend to examine a closed loop control system in future research which can continuously re-estimate and re-predict.

ACKNOWLEDGMENT

This work has been supported by Ausgrid and the Australian Research Council (ARC).

REFERENCES

- [1] 3GPP TR 25.913 V8.0.0 (2008-12), "Requirements for Evolved UTRA (E-UTRA) and Evolved UTRAN (E-UTRAN)", Release 8
- [2] Jason Brown and Jamil Y. Khan, "Performance Comparison of LTE FDD and TDD Based Smart Grid Communications Networks for Uplink Biased Traffic", Smart Grid Communications (SmartGridComm), 2012 IEEE International Conference on, 5-8 Nov. 2012
- [3] Jason Brown and Jamil Y. Khan, "Predictive Resource Allocation in the LTE Uplink for Event Based M2M Applications", IEEE International Conference on Communications (ICC) 2013, Beyond LTE-A Workshop, 9 June 2013
- [4] 3GPP TS 36.331 V8.15.0 (2011-09), "Evolved Universal Terrestrial Radio Access (E-UTRA); Radio Resource Control (RRC); Protocol specification", Release 8.
- [5] 3GPP TS 36.321 V8.10.0 (2011-09), "Evolved Universal Terrestrial Radio Access (E-UTRA); Medium Access Control (MAC) protocol specification", Release 8
- [6] 3GPP TS 36.213 V8.8.0 (2009-09), "Evolved Universal Terrestrial Radio Access (E-UTRA); Physical layer procedures", Release 8
- [7] Teixeira, M.A.; Guardieiro, P.R.; "A predictive scheduling algorithm for the uplink traffic in IEEE 802.16 networks," Advanced Communication Technology (ICACT), 2010 The 12th International Conference on , vol.1, no., pp.651-656, 7-10 Feb. 2010
- [8] El Gamal, H.; Tadrous, J.; Eryilmaz, A.; "Proactive resource allocation: Turning predictable behavior into spectral gain," Communication, Control, and Computing (Allerton), 2010 48th Annual Allerton Conference on, Sept. 29 2010-Oct. 1 2010
- [9] Tadrous, J.; Eryilmaz, A.; El Gamal, H., "Proactive Resource Allocation: Harnessing the Diversity and Multicast Gains", Information Theory, IEEE Transactions on, vol.59, no.8, pp.4833-4854, Aug. 2013